

This discussion paper is/has been under review for the journal *Atmospheric Chemistry and Physics (ACP)*. Please refer to the corresponding final paper in *ACP* if available.

**CNR-IMAA
measurements in
correspondence of
CALIPSO overpass**

L. Mona et al.

One year of CNR-IMAA multi-wavelength Raman lidar measurements in correspondence of CALIPSO overpass: Level 1 products comparison

L. Mona, G. Pappalardo, A. Amodeo, G. D'Amico, F. Madonna, A. Boselli, A. Giunta, F. Russo, and V. Cuomo

Consiglio Nazionale delle Ricerche, Istituto di Metodologie per l'Analisi Ambientale (CNR-IMAA), C. da S. Loja, 85050 Tito Scalco, Potenza, Italy

Received: 19 January 2009 – Accepted: 18 March 2009 – Published: 31 March 2009

Correspondence to: L. Mona (mona@imaa.cnr.it)

Published by Copernicus Publications on behalf of the European Geosciences Union.

Title Page

Abstract

Introduction

Conclusions

References

Tables

Figures

⏪

⏩

◀

▶

Back

Close

Full Screen / Esc

Printer-friendly Version

Interactive Discussion

Abstract

At CNR-IMAA, an aerosol lidar system is operative since May 2000 in the framework of EARLINET (European Aerosol Research Lidar Network), the first lidar network for tropospheric aerosol study on continental scale. High quality multi-wavelength measurements make this system a reference point for the validation of data products provided by CALIPSO (Cloud-Aerosol Lidar and Infrared Pathfinder Satellite Observations), the first satellite-borne lidar specifically designed for aerosol and cloud study. Since 14 June 2006, devoted measurements are performed at CNR-IMAA in coincidence of CALIPSO overpasses. For the first time, results on 1-year comparisons between ground-based multi-wavelength Raman lidar measurements and corresponding CALIPSO lidar Level 1 profiles are presented. A methodology for the comparison is presented and discussed into details. Cases with the detection of cirrus clouds in CALIPSO data are separately analysed for taking into account eventual multiple scattering effects. For cirrus cloud cases, few cases are available to draw any conclusions. For clear sky conditions, the comparison shows good performances of the CALIPSO on-board lidar: the mean relative difference between the ground-based and CALIPSO Level 1 measurements is always within its standard deviation at all altitudes, with a mean difference in the 3–8 km altitude range of $(-2 \pm 12)\%$. At altitude ranges corresponding to the typical PBL height observed at CNR-IMAA, a mean underestimation of $(-24 \pm 20)\%$ is observed in CALIPSO data, probably due to the difference in the aerosol content at the location of PEARL and CALIPSO ground-track location. Finally, the mean differences are on average lower for the closest overpasses (at about 40 km), with an increment of the differences at all altitude ranges when the 80 km overpasses are considered.

ACPD

9, 8429–8468, 2009

CNR-IMAA measurements in correspondence of CALIPSO overpass

L. Mona et al.

Title Page

Abstract

Introduction

Conclusions

References

Tables

Figures

⏪

⏩

◀

▶

Back

Close

Full Screen / Esc

Printer-friendly Version

Interactive Discussion

1 Introduction

Tropospheric aerosols, and in particular anthropogenic aerosols, are one of the most uncertain elements in the estimation of radiation budget, in fact the uncertainties in aerosol direct and indirect anthropogenic forcing are of the same magnitude of the effects themselves (Forster et al., 2007). The main cause of uncertainty is the large tropospheric aerosol variability in space and time. It is well known that a coordinated approach of local, regional, and global observations, and physical, chemical, radiation, and dynamics modelling is needed for dramatically improving our understanding of aerosol climate impacts and environmental interactions (Diner et al., 2004). In addition, it has to be considered that in the past, the variability of the horizontal and temporal distribution of aerosols and of their optical properties has been investigated mainly by means of passive remote sensing instruments on board of satellites or ground based sun photometers networks like AERONET (Kaufmann et al., 2000; Anderson et al., 2003; Omar et al., 2005; Kahn et al., 2007). In these studies based on columnar measurements, there are no information about the vertical distribution of the aerosols that is a crucial point for the aerosol-clouds interaction study. Moreover, since vertical concentration gradients can lead also to significant horizontal inhomogeneities, the lack of information about the vertical mixing can be a large source of variability typically neglected in the models.

Aerosol profiling with high resolution both in time and space provided by lidar techniques is an indispensable tool to study the vertical structure of aerosol field and its temporal and spatial evolution. Moreover, lidar techniques can penetrate optically thin clouds allowing, therefore, to investigate aerosol-clouds interactions and the aerosol indirect effects on radiation budget.

Since April 2006, CALIPSO (Cloud-Aerosol Lidar and Infrared Pathfinder Satellite Observations), the first satellite-borne lidar specifically designed for aerosol and cloud study, provides high vertical resolution profiling of aerosol and clouds on global scales (Winker et al., 2007). Flying in the A-train constellation, CALIPSO offers, for the first

**CNR-IMAA
measurements in
correspondence of
CALIPSO overpass**

L. Mona et al.

Title Page

Abstract

Introduction

Conclusions

References

Tables

Figures



Back

Close

Full Screen / Esc

Printer-friendly Version

Interactive Discussion

time, the possibility for developing an integrated strategy between lidar and passive remote sensing techniques thanks to the synergies among different A-train sensors for both aerosols and clouds studies (Stephens et al., 2002; Anderson et al., 2005; Hu et al., 2007; Lamquin et al., 2008; Sassen et al., 2008).

5 CALIOP (Cloud-Aerosol Lidar with Orthogonal Polarization), the lidar on board of CALIPSO, is an elastic backscatter lidar that provides vertical profiles of aerosol and clouds backscatter coefficients at 532 nm and 1064 nm and depolarization ratio profiles at 532 nm. Since the equation for a lidar in the elastic configuration has two unknowns, the extinction and backscatter coefficients, an assumption on their ratio, i.e. the lidar
10 ratio, is needed for retrieving profiles of extinction and backscatter coefficients from the CALIOP measurements. A first guess of the lidar ratio is selected in CALIPSO retrieval algorithms on the type and subtype of the layer being analysed and mainly on the base of AERONET climatological studies and model calculations (Cattrall et al., 2005; Liu et al., 2005; Young et al., 2008). However, it has been observed that even for the
15 same kind of aerosol, the lidar ratio can largely varies because of the natural variability of each aerosol species and of the aerosol modification/transportation processes (Mona et al., 2006; Müller et al., 2007; Müller et al., 2008; Papayannis et al., 2008). In order to increase and validate the accuracy of aerosol optical properties retrieved from CALIPSO pure backscatter lidar, comparisons with ground-based elastic/Raman
20 lidar measurements are strongly necessary, since this technique allows to characterize atmospheric aerosols in terms of vertical profiles of extinction and backscatter coefficients without any assumptions on the aerosol type and composition (Ansmann et al., 1990; Ansmann et al., 1992). However, before proceeding with the comparison on final CALIPSO products (namely the Level 2 products), it is important to study and assess
25 the accuracy of CALIPSO raw signals (Level 1 data). This is essential to identify, if it is the case, possible biases due, for example, to specular reflection, multiple scattering effects, or to low accuracy at some altitude ranges because of low SNR and to the calibration procedure. Only after a check of the unprocessed CALIPSO data, the comparison in terms of Level 2 products will allow to check and improve CALIPSO retrieval

**CNR-IMAA
measurements in
correspondence of
CALIPSO overpass**L. Mona et al.

[Title Page](#)[Abstract](#)[Introduction](#)[Conclusions](#)[References](#)[Tables](#)[Figures](#)[⏪](#)[⏩](#)[◀](#)[▶](#)[Back](#)[Close](#)[Full Screen / Esc](#)[Printer-friendly Version](#)[Interactive Discussion](#)

**CNR-IMAA
measurements in
correspondence of
CALIPSO overpass**

L. Mona et al.

[Title Page](#)[Abstract](#)[Introduction](#)[Conclusions](#)[References](#)[Tables](#)[Figures](#)[⏪](#)[⏩](#)[◀](#)[▶](#)[Back](#)[Close](#)[Full Screen / Esc](#)[Printer-friendly Version](#)[Interactive Discussion](#)

algorithms and assumptions. Comparing first ground-based vs. CALIPSO Level 1 products allows to distinguish problems and biases contained already in the acquired and calibrated lidar signal from uncertainties and errors related to misleading assumptions needed in the optical properties retrieval algorithms. As shown in the present work, a comparison in terms of CALIPSO Level 1 data starting from ground-based measurements is possible without assumptions only if independent extinction and backscatter profiles are available, as it is possible with the elastic/Raman technique.

In this paper, the methodology for addressing this kind of comparison is presented and discussed into details, and, for the first time, a 1-year comparison between ground-based multi-wavelength Raman lidar measurements and corresponding CALIPSO lidar profiles is presented. After a brief description of the CNR-IMAA multi-wavelength lidar system operative within EARLINET (Bösenberg et al., 2000), the methodology for the comparison in terms of CALIPSO Level 1 data is presented. In particular, the status of the correlative measurements acquired at CNR-IMAA since June 2006 following the EARLINET devoted strategy for CALIPSO measurements (Mattis et al., 2007) is presented. Then the procedure for the calculation of profiles to be compared to CALIPSO Level 1 profiles starting from aerosol extinction and backscatter profiles measured by means of the CNR-IMAA lidar is presented and discussed. In the third section a comparison for a strong Saharan dust event is reported as example of the applied methodology. Then results on 1-year of night-time measurements are reported for cirrus cloud cases and clear sky conditions. Finally, conclusions and perspectives are given.

2 Elastic/Raman aerosol lidar system

At the CNR-IMAA, located in Tito Scalco, Potenza (40°36' N, 15°44' E, 760 m above sea level), a Raman lidar system for tropospheric aerosol study is operative since the beginning of EARLINET in May 2000. The Potenza EARLINET lidar (PEARL) is based on a Nd:YAG laser equipped with second and third harmonics generators and on a Cassegrain reflecting telescope with a primary mirror of 500 mm diameter

**CNR-IMAA
measurements in
correspondence of
CALIPSO overpass**

L. Mona et al.

[Title Page](#)[Abstract](#)[Introduction](#)[Conclusions](#)[References](#)[Tables](#)[Figures](#)[⏪](#)[⏩](#)[◀](#)[▶](#)[Back](#)[Close](#)[Full Screen / Esc](#)[Printer-friendly Version](#)[Interactive Discussion](#)

and combined focal length of 5 m. The three laser beams at 1064, 532 and 355 nm are simultaneously and coaxially transmitted into atmosphere after they are separately expanded. The receiving system has 3 channels for the detection of the radiation elastically backscattered from the atmosphere at the 3 laser wavelengths and two channels for the detection of the Raman radiation backscattered from the atmospheric N₂ molecules at 607 and 386 nm. An additional Raman channel at 407 nm collects radiation backscattered from the water vapor molecules present in the atmosphere. Finally a cubic polarizing beam splitter allows the detection of components of backscattered light polarized perpendicular and parallel to the direction of the linearly polarized transmitted laser beam. The backscattered radiation collected by the telescope is spectrally selected by means of dichroic mirrors and interferential filters with a bandwidth of 0.5 nm. After spectral selection, the signal at each wavelength is furthermore split in two signals of different intensity by means of a beam splitter. This allows to obtain a lidar signal extending from low altitude range to the free troposphere with a good statistic and overcoming the detector limited counting scale interval.

PEARL allows independent measurements of the aerosol extinction and backscatter coefficients, and therefore of the lidar ratio at 532 nm and 355 nm, thanks to the combined elastic/Raman approach (Ansmann et al., 1990, Ferrare et al., 1998). An iterative approach (Di Girolamo et al., 1999) is used for retrieving the aerosol backscatter coefficient at 1064 nm starting from the elastically backscattered lidar signal at this wavelength and assuming a lidar ratio profile at 1064 nm, on the basis of literature values and simultaneous lidar ratio measurements at 532 and 355 nm.

With this lidar system, it is possible to measure vertical profiles of aerosol optical properties from low troposphere to the upper troposphere. The full overlap between the transmitted laser beam and the telescope field of view for this system is reached at about 0.8 km above the lidar station. However, the elastic/Raman method for the determination of the aerosol backscatter coefficient profile at 355 and 532 nm involves the ratio of two lidar signals, therefore the overlap effect is partially corrected and these profiles typically start from 400 m above the ground. For the other products, a correc-

tion for the incomplete overlap (Wandinger et al., 2002) is applied and this allows to obtain profiles of the aerosol extinction coefficient at 532 nm and 355 nm and of the aerosol backscatter coefficient at 1064 nm that typically start from 500 m above the lidar station.

Aerosol optical properties vertical profiles are typically obtained by 30 min of temporal integration, and with an effective vertical resolution of 60 m for the aerosol backscatter coefficient and ranging between 60 and 240 m for the aerosol extinction coefficient and lidar ratio. With these resolutions, in night time conditions, typical statistical errors due to the signals detection in the PBL are below 5% for the aerosol backscatter coefficients at 355 and 532 nm, and below 10% for the extinction coefficients at 355 nm and 532 nm. In the free troposphere, typical statistical errors are below 30% for aerosol backscatter at 355 and 532 nm and aerosol extinction, for values of the aerosol extinction at 532 nm higher than about 0.03 km^{-1} . Both the system and the used algorithms have been quality checked and are object of continuous standard checks within the EARLINET Quality Assurance program (Matthias et al., 2004; Böckmann et al., 2004; Pappalardo et al., 2004; Amodeo et al., 2007).

3 PEARL vs. CALIPSO comparison methodology

3.1 Measurements strategy

Because of its Raman multi-wavelength capability, PEARL is an high quality reference point for CALIPSO measurements of the aerosol backscatter coefficient at 532 and 1064 nm. In particular, the PEARL simultaneous measurements of aerosol extinction and backscatter profiles at 532 nm allow to quantify the errors on the CALIPSO backscatter profiles due to lidar ratio assumptions and therefore to improve the algorithms for these retrievals. Furthermore, PEARL aerosol extinction and backscatter measurements at 355 nm, and water vapor mixing ratio profiles, add useful information about microphysical aerosol properties that can be used to improve the retrieval of

Title Page

Abstract

Introduction

Conclusions

References

Tables

Figures

◀

▶

◀

▶

Back

Close

Full Screen / Esc

Printer-friendly Version

Interactive Discussion

aerosol backscatter coefficient from pure backscatter lidar.

Since 14 June 2006, devoted measurements are performed at CNR-IMAA in coincidence of CALIPSO overpasses according to the scientific CALIPSO team requests for the validation purposes. Measurements are performed each time that CALIPSO overpasses PEARL's location within a maximum distance of 100 km and 2 h. Additional measurements are performed in agreement with EARLINET specific strategy designed for the CALIPSO measurements (Mattis et al., 2007). The network measurements plan is distributed to all stations once per week, including, for each station, measurements with CALIPSO overpass within 100 km (Case1) and additional measurements when the EARLINET closest station and the multi-wavelength EARLINET closest station perform measurements in coincidence with CALIPSO (respectively Case2 and Case3). This kind of measurements were suggested for exploiting the EARLINET network capability to investigate aerosol properties modification over the European continent and for combining all these information with CALIPSO profiles. In the following, only Case 1 measurements will be considered because these measurements allow the point-to-point comparison between ground-based and satellite-borne lidar measurements, that is the aim of the current paper.

Following this strategy of measurements, 68 measurements were performed at CNR-IMAA as Case 1 in the June 2006–June 2007 period, covering 77% of the Case 1 measurements scheduled for our station. For these measurements the average minimum distance between PEARL and CALIPSO is of 66.5 km, reaching an absolute minimum distance of 40.3 km. Figure 1 reports two examples of night-time CALIPSO overpasses over Potenza, examples representative of the 2 typical overpasses with a minimum distance of about 40 and 80 km.

3.2 Attenuated backscatter comparison

Ground-based lidar measurements at 3+2 wavelengths are an optimal tool for validation of CALIPSO products, because they provide independent measurements of the particles backscatter and extinction at 532 nm and backscatter at 1064 nm profiles that

**CNR-IMAA
measurements in
correspondence of
CALIPSO overpass**

L. Mona et al.

Title Page

Abstract

Introduction

Conclusions

References

Tables

Figures

⏪

⏩

◀

▶

Back

Close

Full Screen / Esc

Printer-friendly Version

Interactive Discussion



can be directly compared to analogous quantities derived from CALIPSO. However, before these comparisons, it is necessary to assess the quality of CALIPSO Level 1 data in order to distinguish problems and possible biases contained in the acquired lidar signal from uncertainties and errors related to the retrieval algorithms.

5 The main product contained in the CALIPSO Level 1 data is the attenuated backscatter profile, i.e. its range corrected lidar signal unless of a calibration constant (Hostetler et al., 2006).

The attenuated backscatter coefficient β' provided by CALIPSO is defined at each altitude z as (Hostetler et al., 2006):

$$10 \quad \beta'(z) = \beta^{\text{tot}}(z)T_{\text{par}}^2(z)T_{\text{mol}}^2(z)T_{\text{O}_3}^2(z) \quad (1)$$

where β_{tot} is the backscatter coefficient resulting from particles, molecular and ozone contributions:

$$\beta^{\text{tot}}(z) = \beta_{\text{par}}(z) + \beta_{\text{mol}}(z) + \beta_{\text{O}_3}(z) \quad (2)$$

15 and $T_{\text{mol}}^2(z)$, $T_{\text{O}_3}^2(z)$ and $T_{\text{par}}^2(z)$ are the transmission terms present in the elastic lidar equation due respectively to the molecules, ozone and particles contained in the atmosphere layer extending between the lidar and the range z .

The attenuated backscatter profiles provided by CALIPSO are not directly comparable to PEARL profiles, but a procedure has to be followed in order to compare PEARL and CALIPSO independent measurements. In retrieving attenuated backscatter profile from PEARL data, it has to be taken into account that PEARL and CALIPSO transmission terms are different, because the first lidar is an upward looking lidar and CALIPSO is a downward looking lidar. The molecular terms in (1), both backscatter coefficient and transmission, can be obtained by a co-located radiosounding if available or can be well approximated using modelled atmosphere. The ozone terms can be estimated starting from ozone profiles available directly as met data embedded in CALIPSO Level 1 products and taking into account the ozone absorption at 532 nm in the Chappuis band (Brasseur and Solomon, 1985).

[Title Page](#)
[Abstract](#)[Introduction](#)[Conclusions](#)[References](#)[Tables](#)[Figures](#)[I◀](#)[▶I](#)[◀](#)[▶](#)[Back](#)[Close](#)[Full Screen / Esc](#)[Printer-friendly Version](#)[Interactive Discussion](#)

[Title Page](#)[Abstract](#)[Introduction](#)[Conclusions](#)[References](#)[Tables](#)[Figures](#)[⏪](#)[⏩](#)[◀](#)[▶](#)[Back](#)[Close](#)[Full Screen / Esc](#)[Printer-friendly Version](#)[Interactive Discussion](#)

The particles backscatter coefficient in (1) is measured by upward looking PEARL system. The particles transmission term can be calculated from PEARL measurements using the independent measurements of particles extinction profiles. In fact, the particles transmission term for a downward looking lidar can be written as function of the particles extinction:

$$T_{\text{par}}^2(z) = \exp \left(-2 \int_z^{z_s} \alpha_{\text{par}}(\zeta) d\zeta \right) \quad (3)$$

where z_s indicates the satellite-borne lidar altitude.

Therefore, starting from simultaneous and independent measurements of aerosol backscatter and extinction profiles measured by PEARL, it is possible to calculate the CALIPSO-like attenuated backscatter (CLAB) profile at 532 nm without any assumptions.

3.2.1 The molecular profile

As reported above, PEARL measurements allow to calculate the CALIPSO-like attenuated backscatter if the ozone and molecular terms in the equation (1) are calculated starting from radiosoundings or models. In this paragraph we explicitly deal with these molecular terms calculation and their influences on the retrieved CLAB uncertainties.

The ozone terms contribution on the CLAB calculation is around 3% in the 0–10 km a.s.l. and lower above. Considering that the ozone profile is not highly variable, differences due to the ozone profile used for the CLAB calculation can be considered negligible. In the following, for each attenuated backscatter profile comparison, the corresponding ozone profile available directly as met data embedded in CALIPSO Level 1 products is used.

More relevant is the contribution of the molecular terms in (1), that can be exactly calculated if vertical temperature and pressure are known, using Bucholtz's approach (Bucholtz, 1995). This method requires as input the vertical profiles of pressure and

**CNR-IMAA
measurements in
correspondence of
CALIPSO overpass**L. Mona et al.

[Title Page](#)[Abstract](#)[Introduction](#)[Conclusions](#)[References](#)[Tables](#)[Figures](#)[⏪](#)[⏩](#)[◀](#)[▶](#)[Back](#)[Close](#)[Full Screen / Esc](#)[Printer-friendly Version](#)[Interactive Discussion](#)

temperature. For our purposes, simultaneous and lidar co-located measurements of these quantities, for example with radiosoundings, would be obviously the best solution. However, this is not always possible, also because of the expensive cost of radiosondes launch and of the sparse temporal sampling of these measurements. Therefore, alternative solutions have to be explored. The most common way to proceed is to use US standard atmosphere profiles (US Standard Atmosphere, 1976). These profiles are typically used in a satisfying way also for the calculation of the density profiles needed for the aerosol backscatter and extinction retrieval starting from lidar measurements (see for example Ansmann et al., 1990; Ansmann et al., 1992).

Significant differences can be observed, especially in the temperature, between the true atmospheric profile and the corresponding standard atmosphere one. This is evident in Fig. 2, where temperature profile as measured with a radiosonde launched at CNR-IMAA on 20 October 2005, 18:00 UTC and the corresponding standard atmosphere profile are reported. In the troposphere differences up to 3–4 K are observed and a difference of about 10 K is observed in the 15–20 km altitude range.

A better estimation of the temperature profile is provided by NOAA model profiles available at www.arl.noaa.gov, where meteorological products for any location in the world are provided through the GDAS (Global Data Assimilation System) operational system run by NCEP (NOAA National Centers for Environmental Prediction). Figure 2 shows a very good agreement between NOAA modelled radiosounding temperature profile and the true state of the atmosphere measured by CNR-IMAA radiosounding. The vertical resolution of this modelled radiosounding is obviously lower and temperature gradients as that observed on 20 October 2005 at about 11.5 km a.s.l. cannot be caught by NOAA model.

A systematic comparison between radiosondes and NOAA modelled temperature vertical profiles has been carried out using all available CNR-IMAA radiosounding profiles for the 2005 (68 cases). The mean difference is very close to zero (0.03 ± 0.07 K) and lower than 0.2 K in the 0–10 km altitude range. In addition, the profile-to-profile difference never exceeds 2.5 K in the 0–10 km range. On the base of this analysis,

we can affirm that if radiosounding data are not available, NOAA modelled profiles are preferred to the simply standard atmosphere profiles. At this point, it is interesting to quantify how large is the influence of this choice on the attenuated backscatter as retrieved from a ground-based lidar.

For the period June 2006–June 2007, no CNR-IMAA radiosounding profiles are available, therefore we limit the comparison to the NOAA modelled radiosounding and the US standard atmosphere model. For all considered cases, the CALIPSO like attenuated backscatter at 532 nm is calculated starting from the aerosol extinction and backscatter profiles measured by PEARL using the NOAA modelled temperature and pressure profiles and the US standard atmosphere profiles for the calculation of the molecular terms in (1). Then, for each case, the difference between the CLAB profiles obtained with the two different modelled atmosphere profiles is calculated. The mean CLAB difference profile, in percentage, is reported in Fig. 3 as thick line. On the whole profile, the mean difference is on average of about 1%, with lowest values below 4 km a.s.l. (lower than 0.5% in absolute value) and however lower than $\pm 1\%$ up to 11 km a.s.l. Larger values are observed for higher altitudes where the aerosol contribution is typically negligible and therefore the molecular terms prevail. However, the difference in CLAB due to the modelled atmosphere is lower than 2.5% on average also at altitude of about 12 km staying however below the statistical error, typically of about 20%, of PEARL ground-based CLAB profiles at this altitude. The minimum and maximum observed differences in CLAB profiles are reported as thin lines in Fig. 3, together with mean difference profile. Even in the worst cases the influence of modelled atmospheric temperature and pressure profile choice is well below 5% up to 10 km, reaching the highest values of 10% only at 11–12 km.

Our analysis allows us to affirm that, if radiosonde profiles are not available, the NOAA modelled profiles have to be preferred to the standard atmosphere profiles, but that for a statistical analysis in terms of attenuated backscatter comparison with CALIPSO data the influence of the chosen atmosphere description is negligible (typically below 1%). In cases of single profile comparison instead, the differences can

**CNR-IMAA
measurements in
correspondence of
CALIPSO overpass**

L. Mona et al.

Title Page

Abstract

Introduction

Conclusions

References

Tables

Figures

⏪

⏩

◀

▶

Back

Close

Full Screen / Esc

Printer-friendly Version

Interactive Discussion



be larger especially above 10 km a.s.l., therefore for this kind of investigation the assumption about atmospheric density profile is more critical for the calculation of the molecular terms in (1). In the following, NOAA modelled radiosounding data are used, because of their better performances respect to the standard atmospheric profiles.

5 4 An example of comparison

In order to show the capability of PEARL for CALIPSO validation purposes and the comparison methodology, one example of comparison is presented in the following. A major case of Saharan dust intrusion over Europe is considered. NOAA Hysplit back-trajectory analysis (Fig. 4a) shows air masses reaching CNR-IMAA around 3–4 km a.s.l. coming from Southern Spain where in the previous day a large amount of dust was observed, as shown in the MODIS image of 12 August 2006 (Fig. 4b).

The procedure reported in the previous section has been applied to retrieve the CALIPSO-like attenuated backscatter at 532 nm, starting from 3+2 PEARL profiles measured on 13 August 2006, 00:55–01:25 UTC (Fig. 5). It is evident that CALIPSO vertical profile is highly noisy if compared to the PEARL one. In fact in the CALIPSO algorithms an additional averaging is necessary for the identification of vertical layers reaching also a maximum horizontal averaging of 80 km (Vaughan et al., 2005). However, the main layering characteristics are evident also in the 5-km horizontal resolution CALIPSO profile reported in Fig. 5 and these are similar to what observed by the ground-based lidar.

Starting from the ground, there is a sharp decrease around 1.5 km a.s.l. in the CALIPSO profile, clear signature of the PBL top, with a residual layer extending up to about 2.5 km, as shown by the almost vertically homogeneous layer observed by the 2 systems. In the free troposphere a wide layer extends between 2.5 and 5 km a.s.l. Nevertheless, there are differences in the vertical distribution of the aerosol in the Saharan dust layer. These differences in the free troposphere are to be mainly ascribed to the atmospheric variability, that cannot be neglected as demonstrated by

CNR-IMAA measurements in correspondence of CALIPSO overpass

L. Mona et al.

Title Page

Abstract

Introduction

Conclusions

References

Tables

Figures

⏪

⏩

◀

▶

Back

Close

Full Screen / Esc

Printer-friendly Version

Interactive Discussion

the temporal and spatial variations shown in the CALIPSO and PEARL quick-looks reported in Fig. 6a and b, respectively, and to the minimum distance of 44.16 km between CALIPSO ground-track and CNR-IMAA and the difference in time resolution of the two measurements for the reported case. Finally, a cirrus cloud around 9 km a.s.l. is evident in PEARL data but it is not observed in CALIPSO measurements. Looking at Fig. 6b, it is clear that on this day there is a broken cirrus cloud situation, therefore CALIPSO does not catch the cirrus cloud because of horizontal distance between the two sensors.

5 Results

For a quantitative comparison between ground-based and CALIPSO lidar data in terms of attenuated backscatter, we selected, among all measurements performed at CNR-IMAA in correspondence of CALIPSO overpass, night-time cases, because, in absence of the solar background, it is possible to obtain independent measurements of backscatter and extinction coefficients vertical profiles at 532 nm and therefore a CALIPSO-like attenuated backscatter profile at the same wavelength using the method reported in Sect. 3.2.

CALIPSO Level 1 data of Version V2.01 are used. Attenuated backscatter profiles are provided in Level 1 data with the original resolution of 1/3 km. In order to reduce the noise in the CALIPSO signal, profiles are averaged on an horizontal scale of 5 km, accordingly to horizontal resolution of CALIPSO Level 2 Layer Aerosol products (Vaughan et al., 2008). The typical horizontal distance between PEARL and CALIPSO ground-track is of about 60 km with a minimum distance of 40.3 km. Profiles are almost coincident in time, because PEARL temporal integration window (typically 30 min) is centred around the CALIPSO overpass over Potenza. Following the procedure reported in Sect. 3.2, CLAB is calculated starting from backscatter and extinction profiles and using ozone profiles embedded in met CALIPSO Level 1 and the molecular profiles calculated starting from the NOAA modelled radiosounding data. After CLAB calcu-

Title Page

Abstract

Introduction

Conclusions

References

Tables

Figures



Back

Close

Full Screen / Esc

Printer-friendly Version

Interactive Discussion



lation, PEARL vertical profiles resolution is degraded to the CALIPSO lower resolution, through linear interpolation, for allowing a quantitative comparison between the CALIPSO and PEARL datasets.

Low clouds cases have been identified in PEARL measurements and removed for the comparison reported in this work, because the high variability of low clouds fields and the typical horizontal distance between the 2 sampled air volumes would bias the study.

In this way among the 31 nights when PEARL performed measurements in coincidence of CALIPSO overpasses, we selected 22 cases in absence of low clouds. In 3 cases CALIPSO data are not available and in 3 cases PEARL vertical profiles of particulate extinction are not available. Finally 16 cases are available for the comparison.

Figure 7 reports the mean, over the 16 cases, vertical profiles of attenuated backscatter as measured by CALIPSO and obtained by PEARL data. There is a good agreement between the two observations, even if there are some differences especially in the PBL and at high altitudes where signatures of cirrus clouds are evident. There is a strong peak in CALIPSO data around 2.5 km a.s.l., signature of very low cloud. The corresponding 2 cases are removed in the analysis reported in the following.

Large differences observed in the PBL region, typically below 2.5 m a.s.l. at our station (Pandolfi et al., 2004; Mona et al., 2006), and at low altitudes are probably due to the distance between the location of PEARL and the CALIPSO ground-track, that is always larger than 40 km and to the CALIPSO horizontal resolution of 5 km. In this context, it is also to be considered that the Potenza lidar station is located at 760 m a.s.l. with a complex horography of the surrounding area that makes very difficult the comparison in the PBL with satellite data acquired with no-perfect spatial coincidence. However, it has to be taken into account that specular reflection from the ground in the CALIPSO nadir configuration can influence these low altitudes measurements.

The difference between satellite and ground-based observations reaches also 100% between 8 and 11 km a.s.l. in the cirrus region. A better agreement is achieved in the altitude range between 3 and 8 km, where however it seems that CALIPSO slightly

**CNR-IMAA
measurements in
correspondence of
CALIPSO overpass**

L. Mona et al.

Title Page

Abstract

Introduction

Conclusions

References

Tables

Figures



Back

Close

Full Screen / Esc

Printer-friendly Version

Interactive Discussion



underestimates the direct ground-based measurements. These could be an effect of the presence of cirrus cases, with different geometrical and optical extension in the PEARL and CALIPSO observations. Therefore cirrus and no cirrus cases are analysed separately in the following.

5.1 Cirrus clouds cases

Among the 14 selected cases, cirrus are observed by PEARL and/or CALIPSO in 5 coincident measurements. However, cirrus are not always detected by both lidars because of the high variability typical of cirrus clouds and of the distance between the air volumes sampled. In particular, cirrus are detected only by PEARL in 2 cases, in just 1 case CALIPSO observes a cirrus not detected by PEARL and finally in 2 cases cirrus clouds are detected by both the ground-based and satellite-borne lidars.

In presence of cirrus clouds, multiple scattering is typically not negligible, in particular for space-borne lidars (Winker, 2003). The main effect of multiple scattering is an apparent extinction and optical depth lower than real one, with an almost unchanged backscatter. For CALIPSO data, multiple scattering influence on Level 1 data have been observed through the comparison with collocated AIRS data (Lamquin et al., 2008) and a multiple scattering correction on Level 2 data is applied for cirrus cloud cases (Liu et al., 2005).

In addition, it is well known that space-borne lidar measurements of ice clouds are typically affected by specular reflection, when observed by lidar at zenith or nadir (Young and Vaughan, 2008). Specular reflection causes anomalously high backscatter, not coupled by any increase in the extinction (Hogan and Illingworth, 2003). Regarding CALIPSO, at the beginning it was nominally pointed in a “near nadir” direction ($\sim 0.3^\circ$ off nadir), while after 28 November 2007, it was pointed 3° off nadir in order to avoid specular reflection effects. Therefore for the time period considered in this study, specular reflection effects cannot be neglected a priori.

Considering these well-known effects for space-borne lidar, here we focus only on cases with cirrus clouds detected by CALIPSO. On the other hand, the 2 cirrus cases

Title Page

Abstract

Introduction

Conclusions

References

Tables

Figures



Back

Close

Full Screen / Esc

Printer-friendly Version

Interactive Discussion



observed only by PEARL have been included in the statistics presented in the next section after a cirrus cloud removing procedure that rescales the calculated attenuated backscatter taking into account the transmittance terms in the cirrus. For the sake of completeness, here we mention that the results presented in the next section do not change significantly if these 2 cases are not included in the statistics.

Before comparing the CALIPSO and PEARL attenuated backscatter profiles for the 3 CALIPSO observed cirrus cases, these profiles have to be rescaled in order to take into account the difference in transmittance terms due to the presence of cirrus clouds with different geometrical and optical extension in the PEARL and CALIPSO observations.

For ground-based measurements, the cirrus contribution to the transmittance term in (3) is calculated starting from the extinction profile. A rescaled attenuated backscatter is obtained dividing the old one for evaluated T^2 term.

For CALIPSO data, cirrus removing procedure is more complicated because Level 1 data have not information about the extinction profiles and for Level 2 products determination some assumptions are needed. Since we are here interested in a direct comparison with Level 1 data avoiding retrieval assumptions, a method to “remove” cirrus from Level 1 data using only Level 1 products is needed. Following Lamquin et al. (2008), the optical depth and the transmittance term due to the presence of the cirrus are estimated comparing the actual attenuated backscatter profile with Level 1 clear sky profiles acquired close in time and space to the analysed profile. In particular, the closest 50 km clear sky scene within 1000 km horizontal distance is chosen like molecular reference. The ratio between the molecular reference and the actual attenuated backscatter just below the cloud provides optical depth and transmittance term of the cirrus (Lamquin et al., 2008). Also for the space-borne lidar, the rescaled attenuated backscatter is obtained dividing the old one for evaluated T^2 term.

After removing clouds by both PEARL and CALIPSO observations, we can finally compare the new rescaled attenuated backscatter profiles. The mean of attenuated backscatter profiles at 532 nm as observed by CALIPSO and PEARL in these 3 cirrus clouds cases are reported in Fig. 8a. Profiles are reported only for altitude ranges

CNR-IMAA measurements in correspondence of CALIPSO overpass

L. Mona et al.

Title Page

Abstract

Introduction

Conclusions

References

Tables

Figures



Back

Close

Full Screen / Esc

Printer-friendly Version

Interactive Discussion

below the minimum identified cirrus base height.

An almost satisfying agreement between the 2 profiles is observed in the 6–8 km a.s.l. altitude range, where a difference of about $(13\pm 31)\%$ is observed, and in this case, as in the previous comparison, below 2.5 km a.s.l. there is a large discrepancy of about $(-23\pm 14)\%$. Larger differences up to 80% (see Fig. 8) are observed instead in cirrus cases at 3–6 km a.s.l., with a CALIPSO overestimation of the attenuated backscatter. The main cause of the observed difference is related to a single case in which aerosol content is highly variable and CALIPSO detected aerosol up to 5 m while we observed a Saharan dust layer up to about 3 km, producing the observed large difference. Discarding this case, as mean in the 3–6 km altitude range, a residual difference of $(14\pm 34)\%$ is obtained, comparable with what obtained in the 6–8 km range. This could be ascribed to the combination of the aerosol variability at these altitudes and a residual contribution of possible multiple scattering effect that leads to an apparent lower extinction and therefore higher transmissivity for the same backscatter, i.e. an apparently increased attenuated backscatter, below the cirrus clouds. On the other hand, specular reflection has to be discarded as cause of the observed large discrepancy at low altitude, because this effect would lead to an increase of the attenuated backscatter at the altitude where the cirrus cloud is located, but it would not influence the lower portion of the profile.

Due to the low number of cirrus cases comparisons, it is not possible at the moment to draw any conclusions about the presence of multiple scattering effect on CALIPSO signal, but it has to be kept in mind the possibility of no negligible effects on the attenuated backscatter in presence of cirrus clouds.

5.2 No cirrus cloud cases

After removing cirrus cloud cases, a total number of 11 night-time coincident measurements is available for comparison between CALIPSO and PEARL observations. Figure 9 reports, for each case, the CALIPSO attenuated backscatter at 532 nm (black lines) as reported in Level 1 V2.01 products and averaged on 5 km as horizontal reso-

Title Page

Abstract

Introduction

Conclusions

References

Tables

Figures

⏪

⏩

◀

▶

Back

Close

Full Screen / Esc

Printer-friendly Version

Interactive Discussion



lution and the almost simultaneous PEARL CLAB profiles obtained with 30 min as temporal averaging (red lines). These cases range between occurrences of high aerosol load in the free troposphere related to Saharan dust intrusions (e.g. 26 June and 13 August 2006) to very clear conditions (29 January 2007), with a good balance between warm and cold seasons cases.

A very good agreement between CALIPSO and PEARL attenuated backscatter profiles is achieved if only these 11 cases are considered. Compared with Fig. 7, the agreement, for these no cirrus cloud cases, between the CALIPSO and PEARL attenuated backscatter mean profiles (Fig. 10a) is improved at all altitude ranges apart from the very low atmosphere below 2.5 km a.s.l., identified as the typical boundary layer top at CNR-IMAA (Pandolfi et al., 2004; Mona et al., 2006). In particular, differences are strongly reduced not only in the altitude range interested by the cirrus cloud presence (8–12 km a.s.l.), but also in the middle range down to 2.5 km a.s.l. The underestimation in CALIPSO attenuated backscatter shown in Fig. 7 in the middle altitude range is significantly reduced when cirrus cloud cases are removed from the statistical analysis.

Figure 10b reports the relative difference of mean CALIPSO attenuated backscatter profiles at 532 nm with respect to the corresponding quantity measured by PEARL. Above the lowest 2.5 km a.s.l., differences are typically within 20% that is the expected error of Level 2 CALIPSO vertical profiles (Winker et al., 2004).

The mean difference of the whole mean profile is around -12% with a standard deviation of about 28%. Even if this value is in agreement with zero within the error, it is largely shifted toward negative values indicating a possible bias in CALIPSO raw signals. In order to better investigate the reason of this apparent underestimation, the relative CALIPSO vs. PEARL difference in the attenuated backscatter is investigated as a function of the altitude range (Fig. 11) and of the CALIPSO-PEARL horizontal distance (Fig. 12).

Figure 11 reports the mean relative difference between CALIPSO and PEARL observations for different atmospheric layers calculated as average on the 11 considered cases. The related standard deviations are reported as error bars. The analysis is

**CNR-IMAA
measurements in
correspondence of
CALIPSO overpass**L. Mona et al.

Title Page

Abstract

Introduction

Conclusions

References

Tables

Figures



Back

Close

Full Screen / Esc

Printer-friendly Version

Interactive Discussion

reported up to 8 km, where the PEARL statistical error is lower than 10%. At higher altitudes, it has to be considered that besides the large ground-based measurements statistical errors, the molecular terms of Eq. (1) strongly influence the CLAB calculation in this free aerosol region. For these reasons, in the following we limit the comparison altitude range below 8 km.

Looking at Fig. 11, it is clear that the negative bias obtained on the whole profile is mainly due to the PBL region, typically below 2.5 km a.s.l., where a relative difference of $(-24 \pm 20)\%$ is observed. As reported above, the comparison at PBL altitudes is not appropriate due to the distance, always larger than 40 km, between CALIPSO ground-track and the CNR-IMAA. Because of the distance and because of the local aerosol content at this altitude range, one could expect a no perfect agreement between the two observations for case-by-case comparison, but due to the large variability of the aerosol field at this altitude, this would result in a mean difference value close to zero with a large observed standard deviation. This is not the case: CALIPSO seems to underestimate the aerosol content in this low range region. This could be due to specular reflection effects from ground in CALIPSO data but it could be also linked to the difference between the location of PEARL and the exact location of the CALIPSO ground-track. For the typical CALIPSO ground-tracks in the Potenza surroundings for night-time overpasses (see Fig. 1), the closest point to CNR-IMAA is located closer than Potenza to the sea and at a lower altitude. Taking into account that Potenza is not an uncontaminated mountain site, but a city with an industrial area surrounded by rural areas located at 760 m a.s.l., this could lead to a PBL top height higher over Potenza rather than over CALIPSO ground-track closest points, and as a consequence, to a higher aerosol load (both extinction and backscatter, i.e. attenuated backscatter) in the altitude range corresponding to PBL for a mountain site rather than for other locations.

At higher altitudes, CALIPSO vs. PEARL differences are typically slightly negative although the two independent observations are always in agreement within their standard deviations.

Between 3 and 8 km, the 1 km mean differences are very close to zero and range

**CNR-IMAA
measurements in
correspondence of
CALIPSO overpass**

L. Mona et al.

Title Page

Abstract

Introduction

Conclusions

References

Tables

Figures



Back

Close

Full Screen / Esc

Printer-friendly Version

Interactive Discussion

**CNR-IMAA
measurements in
correspondence of
CALIPSO overpass**

L. Mona et al.

[Title Page](#)[Abstract](#)[Introduction](#)[Conclusions](#)[References](#)[Tables](#)[Figures](#)[⏪](#)[⏩](#)[◀](#)[▶](#)[Back](#)[Close](#)[Full Screen / Esc](#)[Printer-friendly Version](#)[Interactive Discussion](#)

between -7.5 and 3.6% with a typical standard deviation of 18% . At these altitudes, the mean percentage difference between the ground-based and CALIPSO measured attenuated backscatter (Fig. 10b) is $(-2 \pm 12)\%$. This very small residual difference, in agreement with zero, can be due to the CALIPSO calibration procedure. The observed large standard deviations can be ascribed to the horizontal distance between the volumes sampled by the 2 lidars in conjunction with the variability of the aerosol field at these altitudes where the wind is responsible of fast changes both in time and space (see for example Fig. 6a and b).

In order to further investigate the relationship between the observed differences and the spatial variability in the aerosol field, the difference between CALIPSO and PEARL attenuated backscatter at 532 nm is studied as a function of the horizontal distance between the two sensors. There are two groups of overpasses, one with closest distance around 43 km (5 cases) and a far overpass around 83 km (6 cases), corresponding to the 2 typical ground-tracks reported in Fig. 1. The closest overpass is located at North-East of Potenza, between the Appennines and the Salerno Gulf, while the overpass at about 80 km far from Potenza is much closer to the sea pretty close to a coastal and flat region, the Ionian Sea region.

The mean percentage relative difference between CALIPSO and PEARL attenuated backscatter at 532 nm is reported in Fig. 12 for each one of these 2 overpasses classes for the different atmospheric layers. Also in this cases the standard deviation of the observed values is reported as error bars. Although in agreement with the standard deviation, the mean differences are lower when the closest overpasses are considered, with an increment of the differences at all altitude ranges when the 80 km overpasses are considered. For both 40 and 80 km distances, larger standard deviations are observed typically in the lower atmospheric altitude layers because of the large variability of the aerosol field at these altitudes. For both classes the mean difference observed in the PBL (namely below 2.5 km a.s.l., the typical PBL height as measured at CNR-IMAA) is significantly negative, with lowest values observed for the 80 km overpasses. This furthermore supports our hypothesis that the negative differences observed in the

PBL are strongly affected by the differences between a mountain but polluted site like Potenza, and the Potenza closest ground-track point observed by CALIPSO. In fact, the mean differences in the PBL are larger, in absolute values, when overpasses much closer to the sea are considered.

6 Conclusions and perspectives

For the first time, a 1-year comparison between ground-based multi-wavelength Raman lidar measurements and corresponding CALIPSO lidar profiles is presented. Comparisons are performed in terms of Level 1 data, which are, unless of the calibration constant, the CALIPSO unprocessed data. Through a devoted methodology, described in this work, backscatter and extinction profiles measured by the ground-based lidar can be converted into the attenuated backscatter, which represents the CALIPSO Level 1 product, without critical assumptions. Comparing this quantity to the CALIPSO data measured in coincidence with ground-based measurements allows to identify problems and biases already contained in the CALIPSO lidar signals (like multiple scattering and specular reflection effects or deviations due to calibration procedure) and to discriminate them from uncertainties and errors related to misleading assumptions needed in the optical properties retrieval algorithms. Only after a check of the unprocessed CALIPSO data, the comparison in terms of Level 2 products will allow to check and improve CALIPSO retrieval algorithms and assumptions.

All night-time measurements performed at CNR-IMAA in coincidence (within 100 km and almost simultaneously in time) with CALIPSO overpass have been analysed. Cirrus cloud cases and clear sky cases have been analysed separately.

For cirrus cloud cases observed by CALIPSO, we found a CALIPSO overestimation of the attenuated backscatter of about 80% in the free troposphere. The main cause of the observed difference is related to a single case in which aerosol content is highly variable. Discarding this case, a residual difference is still present in the 3–6 km altitude range. This could be ascribed to the combination of the aerosol variability at these

CNR-IMAA measurements in correspondence of CALIPSO overpass

L. Mona et al.

Title Page

Abstract

Introduction

Conclusions

References

Tables

Figures

⏪

⏩

◀

▶

Back

Close

Full Screen / Esc

Printer-friendly Version

Interactive Discussion

altitudes and possible presence of multiple scattering effects. However, because of the low number of this kind of cases, at the moment it is not possible to draw any conclusions about the presence of multiple scattering effect on CALIPSO signal.

For clear sky conditions, the comparisons show good performances of the CALIPSO on-board lidar. Apart from the PBL region, the mean difference between the ground-based and CALIPSO measured attenuated backscatter is always within its standard deviation at all altitudes, with a mean difference in the 3–8 altitude range of $(-2 \pm 12)\%$. Largely scattered values in the observed differences and the resulting large standard deviation of the mean difference values are the results of the atmospheric variability at the investigated altitudes. At altitude ranges comparable with typical PBL height observed at CNR-IMAA, a systematic underestimation is observed in CALIPSO data of $(-24 \pm 20)\%$. This could be linked to the difference between the location of PEARL and CALIPSO ground-track location: CALIPSO ground-tracks closest point to CNR-IMAA is typically located closer than Potenza to the sea and at a lower altitude. This could lead to a PBL top height higher over Potenza rather than over CALIPSO ground-track closest points, and as a consequence, to a higher aerosol load (both extinction and backscatter, i.e. attenuated backscatter) in the altitude range corresponding to PBL for a mountain polluted site rather than for other locations.

Studying mean percentage differences profiles as a function of the horizontal distances between CALIPSO and PEARL we found that, although in agreement with the standard deviation, the mean differences are significantly lower when the closest overpasses are considered, with an increment of the differences at all altitude ranges when the 80 km overpasses are considered. In particular, within the PBL, the mean difference is $(-21 \pm 26)\%$ and $(-27 \pm 14)\%$, for a distance of about 40 and 80 km, respectively. Since the overpass at about 80 km far from Potenza is pretty close to a coastal and flat region, this furthermore supports the hypothesis that the negative differences observed in the PBL are due to the differences between a mountain but polluted site like Potenza, and the Potenza closest ground-track point observed by CALIPSO.

On the basis of these satisfying results on CALIPSO Level 1 quality, a devoted study

**CNR-IMAA
measurements in
correspondence of
CALIPSO overpass**

L. Mona et al.

Title Page

Abstract

Introduction

Conclusions

References

Tables

Figures

⏪

⏩

◀

▶

Back

Close

Full Screen / Esc

Printer-friendly Version

Interactive Discussion



for the accuracy of CALIPSO aerosol backscatter profiles will be carried on for evaluation and improving of the retrieval algorithms. On the other hand, in order to better address still unclear points, as the possible influence of CALIOP geometry on the PBL data underestimation, all PEARL data will be used in synergy with others EARLINET stations for CALIPSO data validation on continental scale, applying the methodology presented in this paper. Finally after a quality check of CALIPSO Level 1 products, an integrated study of CALIPSO and EARLINET correlative measurements will open new possibilities for spatial (both horizontal and vertical) and temporal variability of aerosol and clouds investigations.

Acknowledgements. The financial support for EARLINET by the European Commission under grant RICA-025991 is gratefully acknowledged. We acknowledge the support of the European Commission through GEOMon Integrated Project under the 6th Framework Programme (contract number FP6-2005-Global-4-036677).

CALIPSO data were obtained from the NASA Langley Research Center Atmospheric Science Data Center. The authors also thank to the CALIPSO QPQ team of the NASA Langley Research Center for the provision of the CALIPSO ground track data. The atmosphere meteorological products are provided by NOAA through (REAL) Real-time Environmental Applications and Display system. We also thank the NOAA Air Resources Laboratory (ARL) for the provision of the HYSPLIT backtrajectory analysis and the NASA Goddard Space Flight Center for provision of MODIS Aqua data.

Finally, the authors want to express their thanks to Mark Vaughan for his invaluable suggestions.

References

Amodeo, A., Mattis, I., Böckmann, C., et al.: A European research infrastructure for the aerosol study on a continental scale: EARLINET-ASOS, Remote Sensing of Clouds and the Atmosphere XII, edited by: Comerón, A., Picard, R. H., Schäfer, K., Slusser, J. R., Amodeo, A., Proc. SPIE, 6745, 67450Y, (2007)-0277-786X/07/\$, 18, doi:10.1117/12.738401, 2007.

Anderson, T. L., Masonis, S. J., Covert, D. S., Ahlquist, N. C., Howell, S. G., Clarke, A. D., and McNaughton, C. S.: Variability of aerosol optical properties derived from in situ aircraft

**CNR-IMAA
measurements in
correspondence of
CALIPSO overpass**

L. Mona et al.

Title Page

Abstract

Introduction

Conclusions

References

Tables

Figures

⏪

⏩

◀

▶

Back

Close

Full Screen / Esc

Printer-friendly Version

Interactive Discussion



measurements during ACE-Asia, *J. Geophys. Res.*, 108, 8647, doi:10.1029/2002JD003247, 2003.

Ansmann, A., Riebesell, M., and Weitkamp, C.: Measurement of atmospheric aerosol extinction profiles with a Raman lidar, *Opt. Lett.* 15, 746–748, 1990.

5 Ansmann, A., Riebesell, M., Wandinger, U., Weitkamp, C., Voss, E., Lahmann, W., and Michaelis, W.: Combined Raman elastic-backscatter lidar for vertical profiling of moisture, aerosol extinction, backscatter and lidar ratio, *Applied Physics B*, 55, 18–28, 1992.

Böckmann, C., Wandinger, U., Ansmann, A., et al.: Aerosol lidar intercomparison in the framework of the EARLINET project. 2 Aerosol backscatter algorithms, *Appl. Opt.*, 43(4), 977–989, 10 2004.

Bösenberg, J. and Matthias, V.: EARLINET: A European Aerosol Research Lidar Network to Establish an Aerosol Climatology, Max-Planck-Institut für Meteorologie, Report No. 348, Hamburg, Germany, September 2003.

Brasseur, G. and Solomon, S.: *Aeronomy of the Middle Atmosphere*, D. Reidel Publishing, Dordrecht, The Netherlands, 156, 1985.

15 Bucholtz, A.: Rayleigh-scattering calculations for the terrestrial atmosphere, *Appl. Opt.*, 34(15), 2765–2773, 1995.

Catrrall, C., Reagan, J., Thome, K., and Dubovik, O.: Variability of aerosol and spectral lidar and backscatter and extinction ratios of key aerosol types derived from selected Aerosol Robotic Network locations, *J. Geophys. Res.*, 110, D10S11, doi:10.1029/2004JD005124, 2005.

20 Di Girolamo, P., Ambrico, P. F., Amodeo, A., Boselli, A., Pappalardo, G., and Spinelli, N.: Aerosol observations by lidar in the nocturnal boundary layer, *Appl. Opt.*, 38(21), 4585–4595, 1999.

Diner, D. J., Ackerman, T., and Anderson, T. L.: PARAGON: An Integrated Approach for Characterizing Aerosol Climate Impacts and Environmental Interactions, *B. American Meteorol. Soc.*, doi:10.1175/BAMS-85-10-1491, 2004.

25 Ferrare, R. A., Melfi, S. H., Whiteman, D. N., Evans, K. D., Poellot, M., and Kaufman, Y. J.: Raman lidar measurements of aerosol extinction and backscattering 2. Derivation of aerosol real refractive index, single-scattering albedo, and humidification factor using Raman lidar and aircraft size distribution measurements, *J. Geophys. Res.*, 103(D16), 19673–19689, 30 1998.

Forster, P., Ramaswamy, V., Artaxo, P., et al.: The Physical Science Basis, Contribution of Working Group I to the Fourth Assessment Report of the Intergovernmental Panel on Climate Change 2007, edited by: Solomon, S., Qin, D., Manning, M., Chen, Z., Marquis, M., Averyt,

**CNR-IMAA
measurements in
correspondence of
CALIPSO overpass**

L. Mona et al.

Title Page

Abstract

Introduction

Conclusions

References

Tables

Figures



Back

Close

Full Screen / Esc

Printer-friendly Version

Interactive Discussion

K. B., Tignor, M., and Miller, H. L., Cambridge Univ. Press, (<http://www.ipcc.ch>), New York, USA, 2007.

Hogan, R. J. and Illingworth, A. J.: The effect of specular reflection on spaceborne lidar measurements of ice clouds, Report of the ESA Retrieval algorithm for EarthCARE project, 2003.

Hostetler, C. A., Liu, Z., Reagan, J., Vaughan, M., Winker, D., Osborn, M., Hunt, W. H., Powell, K. A., and Trepte, C.: Calibration and level 1 data products, in CALIOP algorithm theoretical basis document, NASA Langley Research Center, Hampton, Virginia, USA, April 2006.

Kahn, R. A., Garay, M. J., Nelson, D. L., Yau, K. K., Bull, M. A., Gaitley, B. J., Martonchik, J. V., and Levy, R. C.: Satellite-derived aerosol optical depth over dark water from MISR and MODIS: Comparison with AERONET and implication for climatological studies, *J. Geophys. Res.*, 112, D18205, doi:10.1029/2006JD008175, 2007.

Kaufman, Y. F., Holben, B. N., Tanré, D., Slutsker, I., Smirnov, A., and Eck, T. F.: Will aerosol measurements from Terra and Aqua polar orbiting satellites represent the daily aerosol abundance and properties?, *Geophys. Res. Lett.*, 27, 3861–3864, 2000.

Lamquin, N., Stubernrauch, C. J., and Pelon, J.: Upper tropospheric humidity and cirrus geometrical and optical thickness : Relationships inferred from 1 year of collocated AIRS and CALIPSO data, *J. Geophys. Res.*, 113, D00A08, doi:10.1029/2008JD010012, 2008.

Liu, Z., Omar, A. H., Hu, Y., Vaughan, M. A., and Winker, D. M.: CALIOP Algorithm Theoretical Basis Document, Part 3: Scene Classification Algorithms, tech. rep., available at: <http://www-calipso.larc.nasa.gov/resources/projectdocumentation.php>, 2005.

Matthias, V., Bösenberg, J., Freudenthaler, V., et al.: Aerosol lidar intercomparison in the framework of the EARLINET project. 1 Instruments, *Appl. Opt.*, 43(4), 961–976, 2004.

Mattis I., Mona, L., Müller, D., et al.: EARLINET correlative measurements for CALIPSO, Lidar Technologies, Techniques, and Measurements for Atmospheric Remote Sensing III, edited by: Singh, U. N., Gelsomina Pappalardo, *Proc. SPIE*, 6750, 67500Z, 0277-786X/07/\$18, doi:10.1117/12.7380902007, 2007.

Mona, L., Amodeo, A., Pandolfi, M., and Pappalardo, G.: Saharan dust intrusions in the Mediterranean area: three years of Raman lidar measurements, *J. Geophys. Res.*, 111, D16203, doi:10.1029/2005JD006569, 2006.

Müller D., Ansmann, A., Mattis, I., Tesche, M., Wandinger, U., Althausen, D., and Pisani, G.: Aerosol-type-dependent lidar ratios observed within Raman lidar, *J. Geophys. Res.*, 112, D16202, doi:10.1029/2006JD008292, 2007.

Müller, D., Heinold, B., Tesche, M., et al.: EARLINET Observations of the 14–22-May Long-

**CNR-IMAA
measurements in
correspondence of
CALIPSO overpass**

L. Mona et al.

Title Page

Abstract

Introduction

Conclusions

References

Tables

Figures

⏪

⏩

◀

▶

Back

Close

Full Screen / Esc

Printer-friendly Version

Interactive Discussion

**CNR-IMAA
measurements in
correspondence of
CALIPSO overpass**

L. Mona et al.

[Title Page](#)[Abstract](#)[Introduction](#)[Conclusions](#)[References](#)[Tables](#)[Figures](#)[◀](#)[▶](#)[◀](#)[▶](#)[Back](#)[Close](#)[Full Screen / Esc](#)[Printer-friendly Version](#)[Interactive Discussion](#)

Range Dust Transport Event During SAMUM 2006: Validation of Results From Dust Transport Modelling, accepted for publication on Tellus, September 2008.

Omar, A. H., Won, J.-G., Winker, D. M., Yoon, S.-C., Dubovik, O., and McCormick, M. P.: Development of global aerosol models using cluster analysis of Aerosol Robotic Network (AERONET) measurements, *J. Geophys. Res.*, 110, D10S14, doi:10.1029/2004JD004874, 2005.

Papayannis, A., Amiridis, V., Mona, L., et al.: Systematic lidar observations of Saharan dust over Europe in the frame of EARLINET (2000–2002), *J. Geophys. Res.*, 113, D10204, doi:10.1029/2007JD009028, 2008.

Pandolfi, M., Amodeo, A., Cornacchia, C., Mona, L., and Pappalardo, G.: Three years of Raman lidar measurements of tropospheric aerosol over Potenza in the framework of EARLINET, 22nd ILRC, 12–16 July 2004 Matera, Italy, edited by: Pappalardo, G. and Amodeo, A., SP-561, 2, 853–856, 2004.

Pappalardo, G., Amodeo, A., Pandolfi, M., et al.: Aerosol lidar intercomparison in the framework of the EARLINET project. 3 -Raman lidar algorithm for aerosol extinction, backscatter and lidar ratio, *Appl. Opt.*, 43(28), 5370–5385, 2004.

U.S. Standard Atmosphere, 1976, National Oceanic and Atmospheric Administration – National Aeronautic and Space Administration - United States Air Force, US Government Printing Office, Washington DC, USA, 241 pp., 1976

Vaughan, M. A., Winker, D. M., and Powell, K. A.: CALIOP Algorithm Theoretical Basis Document, Part 2: Feature Detection and Layer Properties Algorithm, Tech. rep., online available at: <http://www.calipso.larc.nasa.gov/resources/projectdocumentation.php>, 2005.

Young, S. A., Winker, D. M., Vaughan, M. A., Hu, Y., and Kuehn, R. E.: CALIOP Algorithm Theoretical Basis Document, Part 4: Extinction Retrieval Algorithms, Tech. rep., online available at: <http://www.calipso.larc.nasa.gov/resources/projectdocumentation.php>, 2008.

Young, S. A. and Vaughan, M. A.: The retrieval of profiles of particulate extinction from Cloud Aerosol Lidar Infrared Pathfinder Satellite Observations (CALIPSO) data: Algorithm description, *J. Atmos. Oceanic Technol.*, accepted 20 December 2008.

Wandinger, U. and Ansmann, A.: Experimental determination of the lidar overlap profile with Raman lidar, *Appl. Opt.*, 41, 511–514, 2002.

Winker, D.: Accounting for multiple scattering in retrievals from space lidar, *Proc. SPIE Int. Soc. Opt. Eng.*, 5059, 128–139, 2003.

Winker, D., Trepte, C., Pelon, J., Garnier, A., Kovacs, T.: CALIOP Science Validation Plan, Tech.

rep., online available at: <http://calipsovalidation.hamptonu.edu/missionplan.htm>, 2004
Winker, D. M., Hunt, W. H., and McGill, M. J.: Initial performance assessment of CALIOP,
Geophys. Res. Lett., 34, L19803, doi:10.1029/2007GL030135, 2007.

ACPD

9, 8429–8468, 2009

**CNR-IMAA
measurements in
correspondence of
CALIPSO overpass**

L. Mona et al.

Title Page

Abstract

Introduction

Conclusions

References

Tables

Figures

⏪

⏩

◀

▶

Back

Close

Full Screen / Esc

Printer-friendly Version

Interactive Discussion

**CNR-IMAA
measurements in
correspondence of
CALIPSO overpass**L. Mona et al.

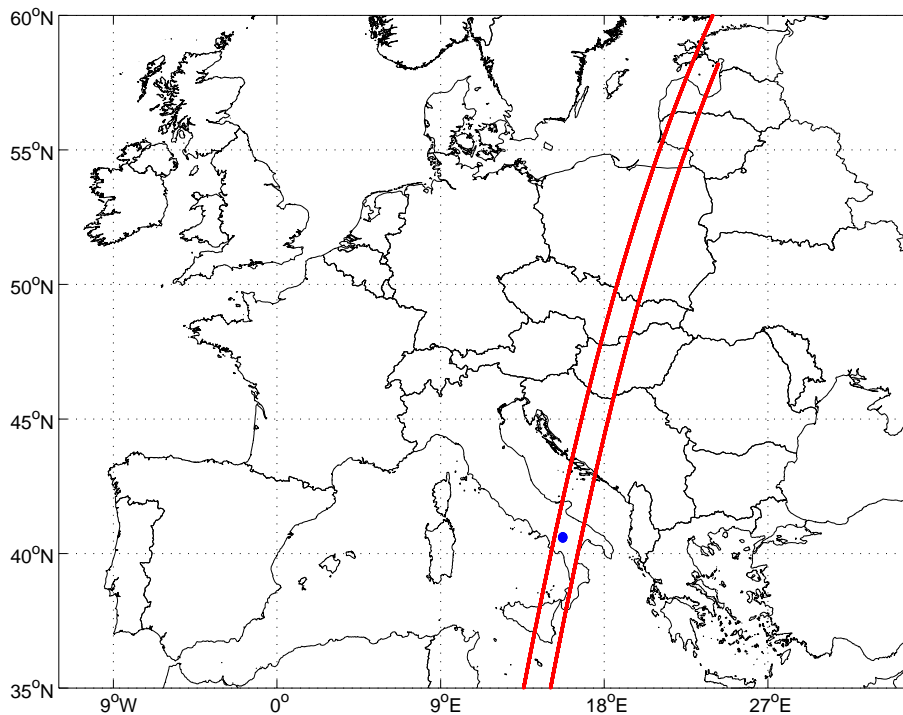


Fig. 1. PEARL location (blue dot) and typical CALIPSO night-time orbits overpassing over Potenza (red lines).

[Title Page](#)[Abstract](#)[Introduction](#)[Conclusions](#)[References](#)[Tables](#)[Figures](#)[◀](#)[▶](#)[◀](#)[▶](#)[Back](#)[Close](#)[Full Screen / Esc](#)[Printer-friendly Version](#)[Interactive Discussion](#)

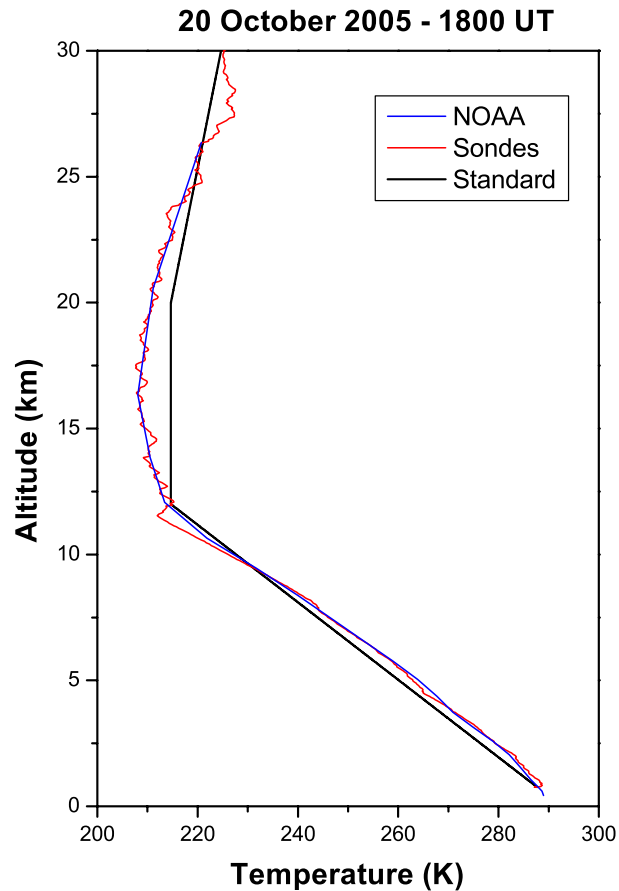


Fig. 2. Temperature profile measured by balloon-borne radiosounding system launched at CNR-IMAA on 20 October 2005, 18:00 UTC (red line). The corresponding US standard atmosphere profile and the NOAA model profiles are reported as black and blue lines, respectively.

**CNR-IMAA
measurements in
correspondence of
CALIPSO overpass**

L. Mona et al.

Title Page

Abstract

Introduction

Conclusions

References

Tables

Figures

◀

▶

◀

▶

Back

Close

Full Screen / Esc

Printer-friendly Version

Interactive Discussion



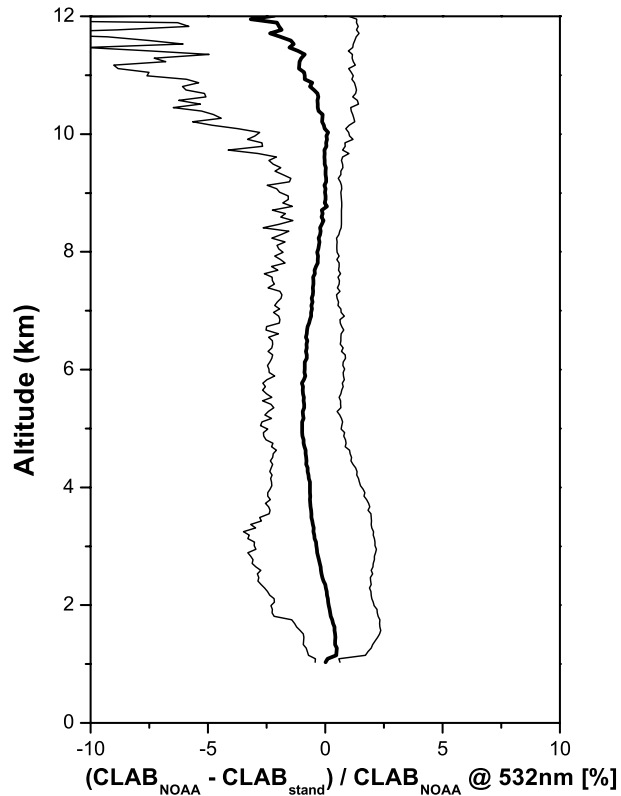


Fig. 3. Difference in CALIPSO like attenuated backscatter (CLAB) resulting by use of NOAA model profile instead of using US atmosphere standard profile. The thick line reports the mean profile calculated over all the selected cases for CALIPSO – PEARL comparison, thin line report the minimum and maximum observed differences in CLAB profiles.

**CNR-IMAA
measurements in
correspondence of
CALIPSO overpass**

L. Mona et al.

Title Page

Abstract

Introduction

Conclusions

References

Tables

Figures

◀

▶

◀

▶

Back

Close

Full Screen / Esc

Printer-friendly Version

Interactive Discussion

CNR-IMAA measurements in correspondence of CALIPSO overpass

L. Mona et al.

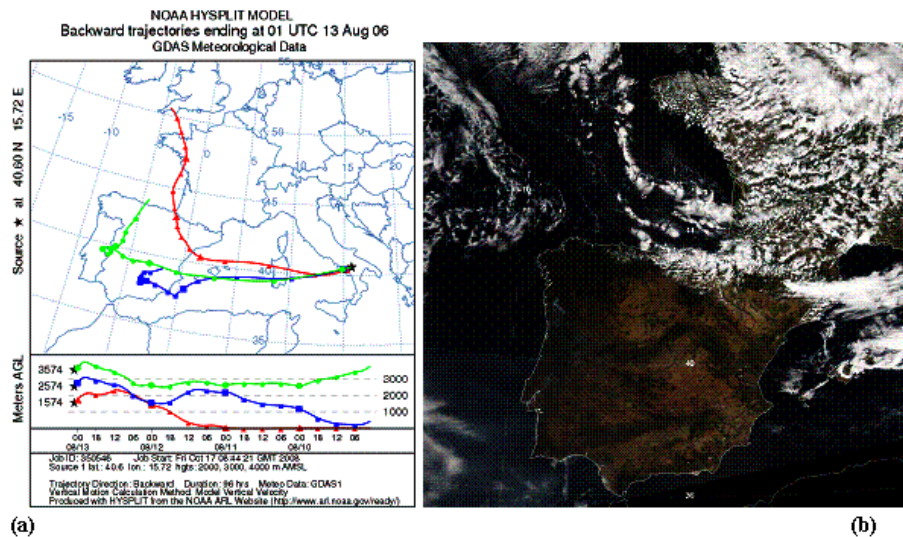


Fig. 4. NOAA Hysplit back-trajectory analysis for 13 August 2006, 01:00 UTC **(a)** and MODIS Aqua image acquired on 12 August 2006, 13:10 UTC **(b)**.

[Title Page](#)
[Abstract](#)
[Introduction](#)
[Conclusions](#)
[References](#)
[Tables](#)
[Figures](#)
[⏪](#)
[⏩](#)
[◀](#)
[▶](#)
[Back](#)
[Close](#)
[Full Screen / Esc](#)
[Printer-friendly Version](#)
[Interactive Discussion](#)

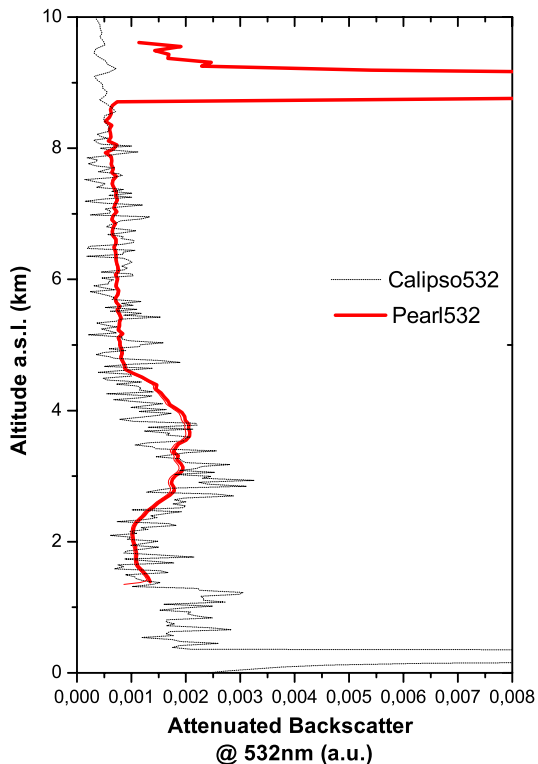


Fig. 5. CALIPSO attenuated backscatter profile at 532 nm measured at 01:11 UTC on 13 August 2006 and corresponding CALIPSO-like profile calculated starting from PEARL profiles measured at 00:55–01:25 UTC on 13 August 2006. The reported CALIPSO attenuated backscatter has an horizontal resolution of 5 km, i.e. it is obtained as the average of 15 single shot attenuated backscatter profiles.

**CNR-IMAA
measurements in
correspondence of
CALIPSO overpass**

L. Mona et al.

Title Page

Abstract

Introduction

Conclusions

References

Tables

Figures

⏪

⏩

◀

▶

Back

Close

Full Screen / Esc

Printer-friendly Version

Interactive Discussion

CNR-IMAA measurements in correspondence of CALIPSO overpass

L. Mona et al.

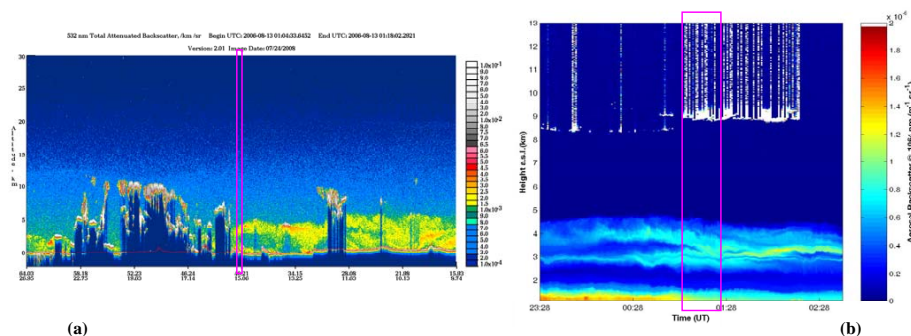


Fig. 6. (a) Temporal evolution of attenuated backscatter vertical profiles measured by CALIPSO at 532 nm on 13 August 2006. (b) Temporal evolution of aerosol backscatter coefficient vertical profiles measured at 1064 nm on 13 August 2006 by PEARL at CNR-IMAA. The vertical and temporal resolution are respectively 7.5 m and 30 s. The purple box indicates the location in space (Fig. 6a) and time (Fig. 6b) of CALIPSO overpass over CNR-IMAA.

Title Page

Abstract

Introduction

Conclusions

References

Tables

Figures

◀

▶

◀

▶

Back

Close

Full Screen / Esc

Printer-friendly Version

Interactive Discussion

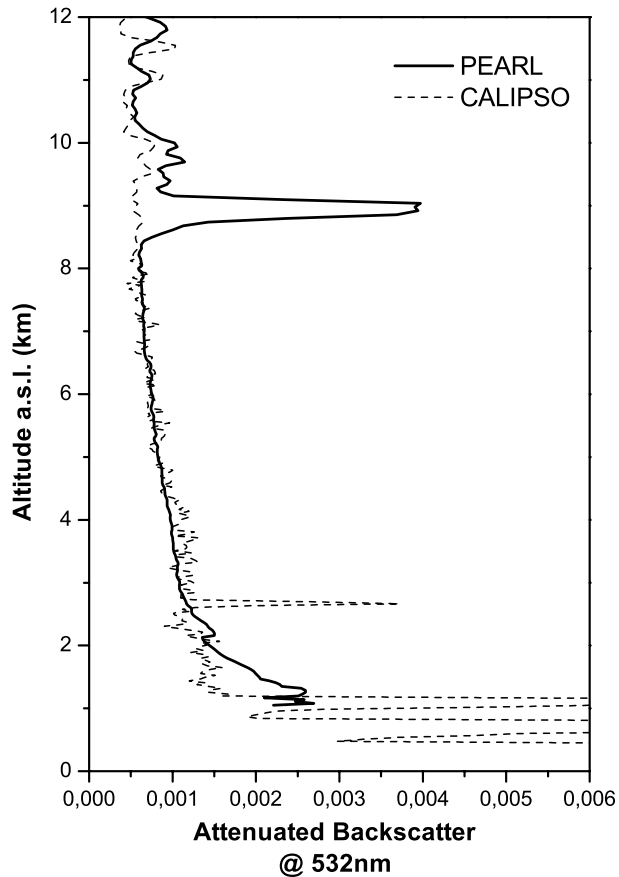


Fig. 7. Mean profiles of attenuated backscatter at 532 nm as measured by CALIPSO and PEARL for all night-time cases, with no-low clouds observed by the CNR-IMAA lidar.

**CNR-IMAA
measurements in
correspondence of
CALIPSO overpass**

L. Mona et al.

Title Page

Abstract

Introduction

Conclusions

References

Tables

Figures

◀

▶

◀

▶

Back

Close

Full Screen / Esc

Printer-friendly Version

Interactive Discussion



CNR-IMAA
measurements in
correspondence of
CALIPSO overpass

L. Mona et al.

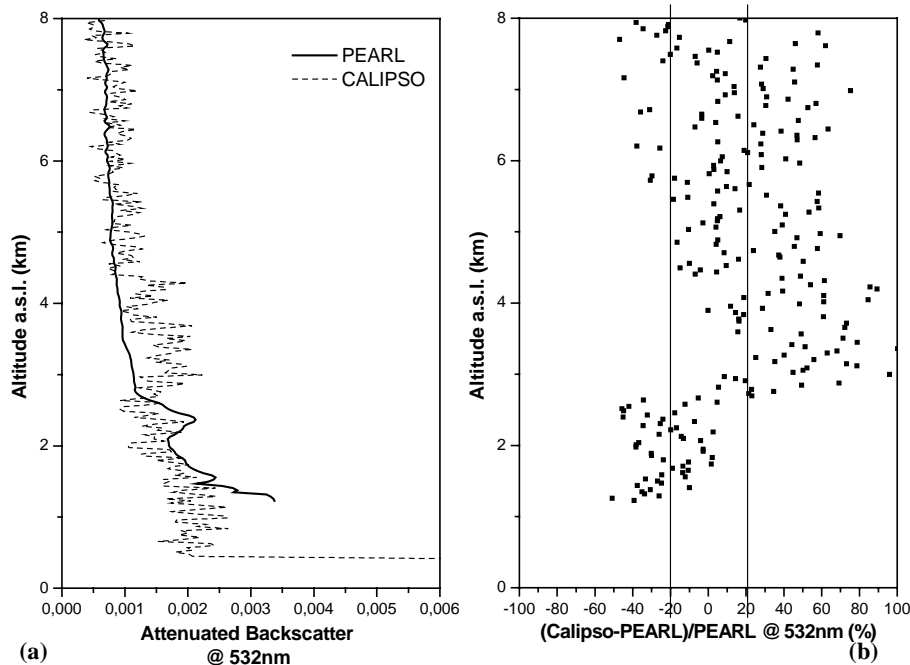
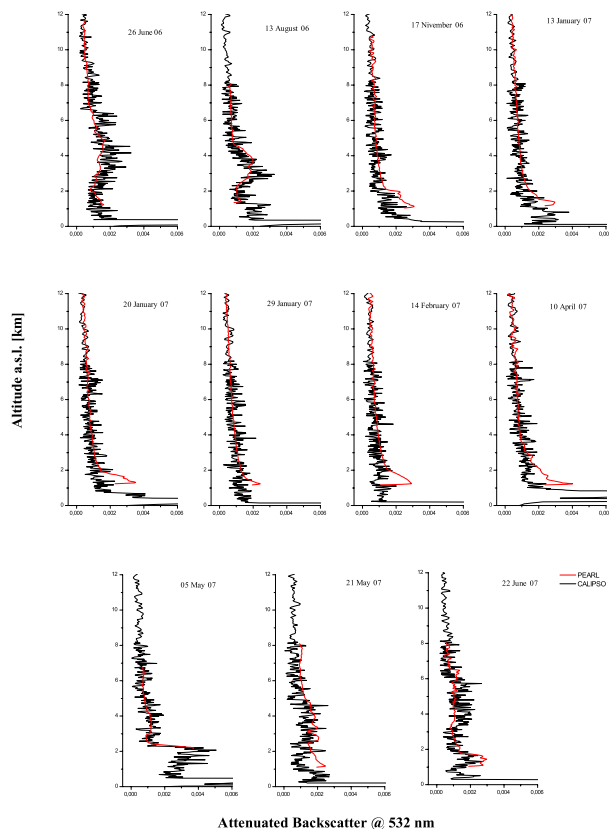


Fig. 8. Comparison between attenuated backscatter at 532 nm as measured by CALIPSO and PEARL for all night-time cases (3) in which CALIPSO detected cirrus cloud: mean attenuated backscatter profiles (a) and mean percentage difference as a function of the altitude (b).

[Title Page](#)[Abstract](#)[Introduction](#)[Conclusions](#)[References](#)[Tables](#)[Figures](#)[◀](#)[▶](#)[◀](#)[▶](#)[Back](#)[Close](#)[Full Screen / Esc](#)[Printer-friendly Version](#)[Interactive Discussion](#)

**CNR-IMAA
measurements in
correspondence of
CALIPSO overpass**

L. Mona et al.



Attenuated Backscatter @ 532 nm

Fig. 9. CALIPSO attenuated backscatter at 532 nm (black lines) for all night-time cases of CALIPSO-PEARL correlative measurements in which no cirrus clouds are detected by CALIPSO. The corresponding PEARL CLAB at 532 nm are reported as red lines. CALIPSO profiles are obtained with 5 km as horizontal resolution. PEARL profiles are average on 30 min centered around the CALIPSO overpass over CNR-IMAA.

[Title Page](#)[Abstract](#)[Introduction](#)[Conclusions](#)[References](#)[Tables](#)[Figures](#)[◀](#)[▶](#)[◀](#)[▶](#)[Back](#)[Close](#)[Full Screen / Esc](#)[Printer-friendly Version](#)[Interactive Discussion](#)

**CNR-IMAA
measurements in
correspondence of
CALIPSO overpass**L. Mona et al.

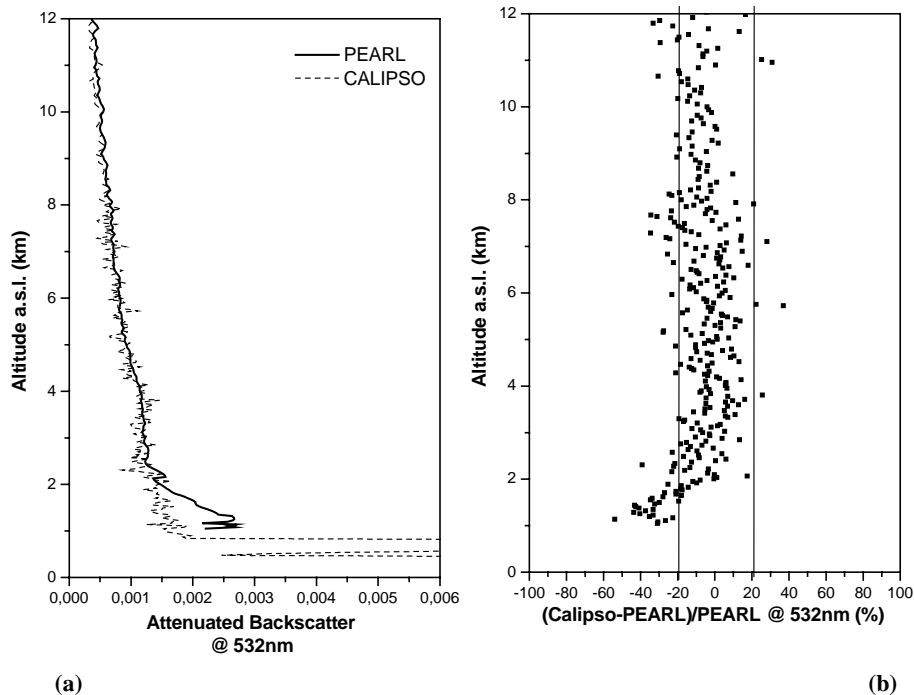


Fig. 10. Comparison between attenuated backscatter at 532 nm as measured by CALIPSO and PEARL for all night-time cases in which no cirrus clouds are detected by CALIPSO: mean attenuated backscatter profiles **(a)** and mean percentage difference as a function of the altitude **(b)**.

[Title Page](#)[Abstract](#)[Introduction](#)[Conclusions](#)[References](#)[Tables](#)[Figures](#)[⏪](#)[⏩](#)[◀](#)[▶](#)[Back](#)[Close](#)[Full Screen / Esc](#)[Printer-friendly Version](#)[Interactive Discussion](#)

**CNR-IMAA
measurements in
correspondence of
CALIPSO overpass**

L. Mona et al.

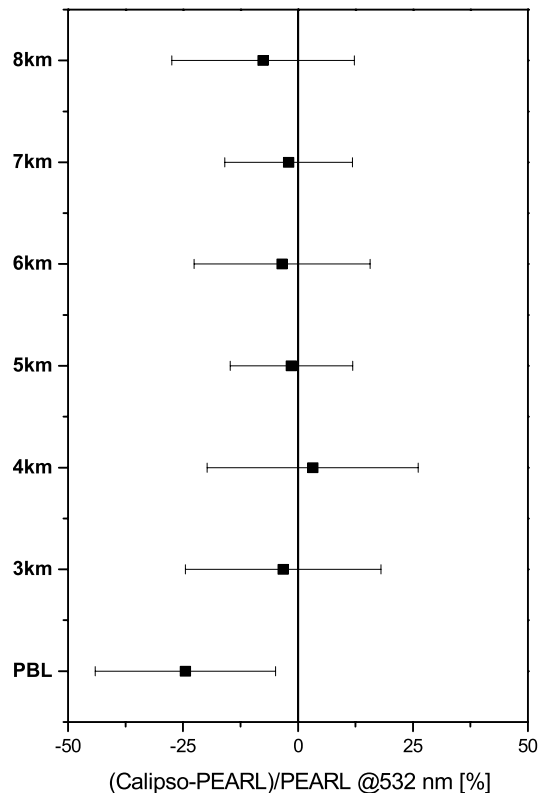


Fig. 11. Mean percentage difference between CALIPSO and PEARL attenuated backscatter at 532 calculated for the PBL region and for the 1km-depth altitude layers extending between 3–8 km for all no cirrus cloud night-time cases. The standard deviation around these mean values are reported as error bars.

[Title Page](#)[Abstract](#)[Introduction](#)[Conclusions](#)[References](#)[Tables](#)[Figures](#)[◀](#)[▶](#)[◀](#)[▶](#)[Back](#)[Close](#)[Full Screen / Esc](#)[Printer-friendly Version](#)[Interactive Discussion](#)

**CNR-IMAA
measurements in
correspondence of
CALIPSO overpass**

L. Mona et al.

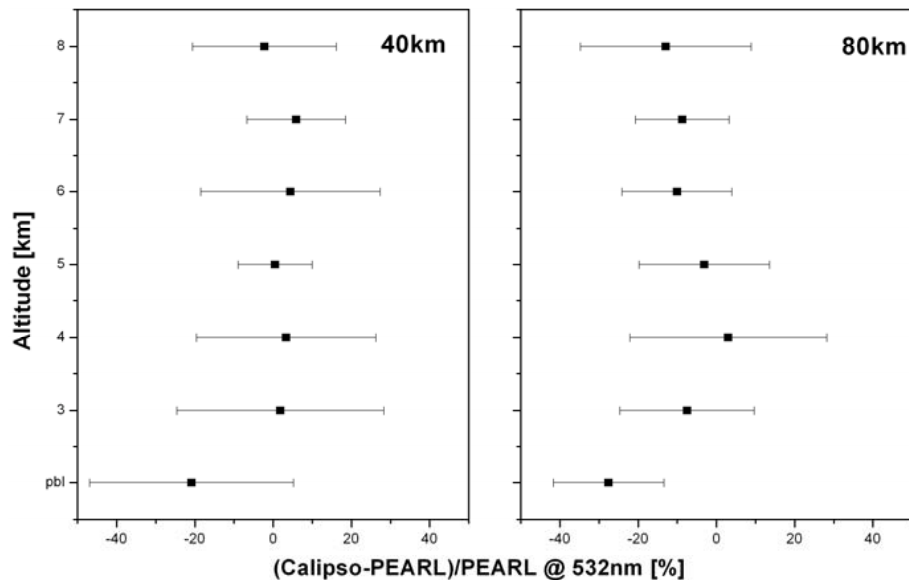


Fig. 12. Mean percentage difference between CALIPSO and PEARL attenuated backscatter at 532 for no cirrus cloud night-time cases divided into two classes: overpasses at about 40 km (left panel) and at about 80 km (right panel). The standard deviation around these mean values are reported as error bars.

[Title Page](#)[Abstract](#)[Introduction](#)[Conclusions](#)[References](#)[Tables](#)[Figures](#)[⏪](#)[⏩](#)[◀](#)[▶](#)[Back](#)[Close](#)[Full Screen / Esc](#)[Printer-friendly Version](#)[Interactive Discussion](#)